energies

MDPI

Article

The Impacts of Reservoir Heterogeneities on the CO_2-Enhanced Oil Recovery Process—A Case Study of Daqingzijing Block in Jilin Oilfield, China

Zetang Li [1,2], Tianfu Xu [1,2,*], Hailong Tian [1,2,*] and Ruosheng Pan [3]

[1] Key Laboratory of Groundwater Resources and Environment, Ministry of Education, Jilin University, Changchun 130021, China; ztli23@mails.jlu.edu.cn
[2] Jilin Provincial Key Laboratory of Water Resources and Environment, Jilin University, Changchun 130021, China
[3] Oil and Gas Engineering Research Institute, CNPC Jilin Oilfield Company, Songyuan 138000, China; panruosheng@163.com
* Correspondence: tianfu_xu@jlu.edu.cn (T.X.); thl@jlu.edu.cn (H.T.)

Abstract: With the exploitation of oilfields, the oil production efficiency of traditional water flooding has been very low, and CO_2-enhanced oil recovery (EOR) has become an inevitable trend of development. CO_2-EOR is affected by many factors, among which the heterogeneity of reservoirs is one of the main influencing factors. In order to understand the impact of different reservoir conditions on the production of oil from CO_2 and the reasons behind it, and on the basis of researching the heterogeneity of reservoir porosity and permeability and its influence on the CO_2-enhanced oil recovery process, this study has altogether established three different reservoir characteristics for comparative analysis. Under the homogeneous and heterogeneous porosity and permeability conditions of a reservoir, the displacement characteristics during a CO_2–oil displacement process were analyzed. The layered heterogenous model had the best oil displacement effect, with its oil displacement amount reaching 8.46×10^4 kg, while the homogeneous model and the spatially heterogenous model had lower values; they were 1.51×10^4 and 1.42×10^4, respectively. The results indicate that the heterogeneous conditions overall improved the flooding effect of CO_2. Under the same injection volume and other reservoir conditions, the cumulative oil flooding effect of the layered heterogenous model was the best compared to the homogeneous and spatially heterogeneous models. Good permeability promotes the accumulation of oil, leading to a higher saturation of the oleic phase. This work provides an in-depth analysis of the effect of the non-uniform distribution of formation permeability on CO_2-enhanced oil recovery and can help to improve carbon sequestration efficiency and oil recovery in CO_2–oil recovery projects.

Keywords: CO_2-enhanced oil recovery; heterogeneity; Jilin Oilfield; numerical simulation

Citation: Li, Z.; Xu, T.; Tian, H.; Pan, R. The Impacts of Reservoir Heterogeneities on the CO_2-Enhanced Oil Recovery Process—A Case Study of Daqingzijing Block in Jilin Oilfield, China. *Energies* **2024**, *17*, 6128. https://doi.org/10.3390/en17236128

Academic Editor: Vladimir Alvarado

Received: 10 October 2024
Revised: 26 November 2024
Accepted: 2 December 2024
Published: 5 December 2024

1. Introduction

The development of the economy and society urgently requires a large amount of fossil fuels such as oil and gas for support [1]. With the exploitation of oilfields, the oil output efficiency of traditional water flooding has been very low, and CO_2-enhanced oil production has become an inevitable trend of development. Under the existing energy structure conditions, CO_2 flooding technology not only increases the output of conventional energy but also stores CO_2. CO_2 flooding technology is relatively mature and has been widely used around the world, such as in the Permian Basin in Texas, USA [2], and the Weyburn oilfield in Saskatchewan, Canada [3]. As early as 1965, China began to explore CO_2 flooding technology in the Daqing oilfield. However, due to various problems, such as insufficient theoretical understanding, poor gas source conditions, and serious gas tampering, China's CO_2 flooding technology developed slowly until 2000 [4–6]. In 2005, Prof. Pingping Shen

first proposed the concept of combining CO_2 flooding with burial storage [4,5]. Since then, China's CO_2 flooding technology has begun to develop gradually. Since the 11th Five-Year Plan (2006–2010), China has set up several national projects including CO_2 storage and resource utilization and has made important progress [4,5]. In September 2020, the "double carbon" goal was proposed, and CCUS-EOR technology began to usher in a period of rapid development opportunities. The combination of CO_2 flooding and CCUS can not only realize the reuse of resources (economic benefits) but also reduce the emission of CO_2 (social benefits). At this stage, many countries are still in the developing phase in this context [4]. CCUS-EOR is not only the main way to reduce carbon emissions on a large scale but also an important way to improve the oil recovery of oilfields [7]. For the above reasons, CCUS-EOR has broad development and application prospects.

However, the process of CCUS-EOR technology is affected by many factors in oilfield blocks, which lead to a limited CO_2 displacement. The heterogeneity of a reservoir is one of the main influencing factors. An in-depth analysis of the mechanism of the non-uniform distribution of formation permeability acting on CO_2–oil production can help to improve the efficiency of carbon sequestration and oil recovery in CO_2–oil production engineering. Since the 1970s, foreign countries have gradually begun research on the influence of heterogeneity on oilfield development. At this stage, the understanding of reservoir heterogeneity is relatively shallow, and the theoretical research is not mature [8].

Around 1960, foreign scholars found the phenomenon of reservoir heterogeneity [9]. In 1990, the heterogeneity of reservoirs was categorized [10], and the principles of its description and analysis were discussed. It was discovered that heterogeneity influences reservoir development and concluded that heterogeneity is always unfavorable to oil recovery [11]. In recent years, the influence of heterogeneity on oilfield development has gradually been paid more attention, and scholars have begun to propose a variety of research methods, among which Yang [12] proposed the heterogeneity composite index method for the first time and established some computational models, which can be regarded as the predecessor of numerical simulation research methods. With the development of science and technology and oil reservoir production methods to increase the oil recovery of oil reservoirs, the research on the heterogeneity of oil reservoirs has become more and more in-depth and detailed. Since 2006, a variety of the effects of heterogeneity on oil recovery have been clarified. The relationship between heterogeneity and residual oil [13], the influence of different fracture directions and depositional rhythms on the oil recovery of CO_2 flooding [14], the influence of the heterogeneity of reservoirs on the mechanism and pattern of oil and gas transportation [15], the influence of vertical and interlayer heterogeneity on recovery [16], or the important influence of reservoir heterogeneity and the injection method on crude oil production [17] are some examples.

Most of the oilfields in China are dominated by terrestrial clastic reservoirs, with complex geological conditions, strong heterogeneity, and large differences in crude oil properties [18]. The research method for reservoirs in China is mainly based on numerical simulation and indoor physical experiments and started later than in other countries. Since 2010, scholars have begun to analyze the influence of different heterogeneity factors on CO_2 flooding by numerical simulation. Through the study of several factors, it has been shown that the stronger the heterogeneity is, the lower the oil recovery of CO_2 flooding is [19–23]. Therefore, some scholars have begun to study how to reduce the impact of reservoir heterogeneity. Liu [24] proposed adjusting well network, well spacing, and injection and production parameters. Kang et al. [25] proposed using polymer gel to improve reservoir heterogeneity. Subsequent studies have found that reservoir heterogeneity can easily lead to the existence of hypertonic channels in their formation, and these channels can lead to gas channels, which in turn can greatly reduce their recovery rate. Therefore, the focus of recent studies has been shifted to gas channels, such as the effect of different replacement pressures and permeability gradients [26,27] on gas channels, and the study of the permeability of tunnels [28].

In general, most of the studies on the effect of reservoir heterogeneity on the oil recovery effect have explored the heterogeneity of two-dimensional reservoirs. On the other hand, regarding three-dimensional reservoirs, heterogeneity caused by sedimentary rhythms has been mainly explored. In this study, we not only set up three different three-dimensional reservoirs for simulation but also set up a spatially heterogenous model to realize the random distribution of permeability and porosity in space. By setting the same injection conditions, the displacement characteristics in the process of CO_2 flooding are investigated. The oil displacement effect of the three models is compared, and the influence of different heterogeneities on the oil displacement effect and the reasons for this effect are analyzed. This study deeply analyzes the influence of different reservoirs on CO_2 flooding and provides technical support for further research on CO_2-EOR and CO_2 sealing stock.

2. Characteristics of the Study Area

In this paper, based on actual stratigraphic conditions and site-measured data, a variety of stratigraphic conditions were designed to investigate the influence of them on CO_2-enhanced oil recovery.

The study area selected for this simulation was the Daqingzi Wells of Jilin Oilfield, which is located in the southern part of the Songliao Basin (Figure 1a), and the main exploration area is shown in Figure 1b. The simulation area selected for this study was Block H59, and the site exploration well deployment map is presented in Figure 1c.

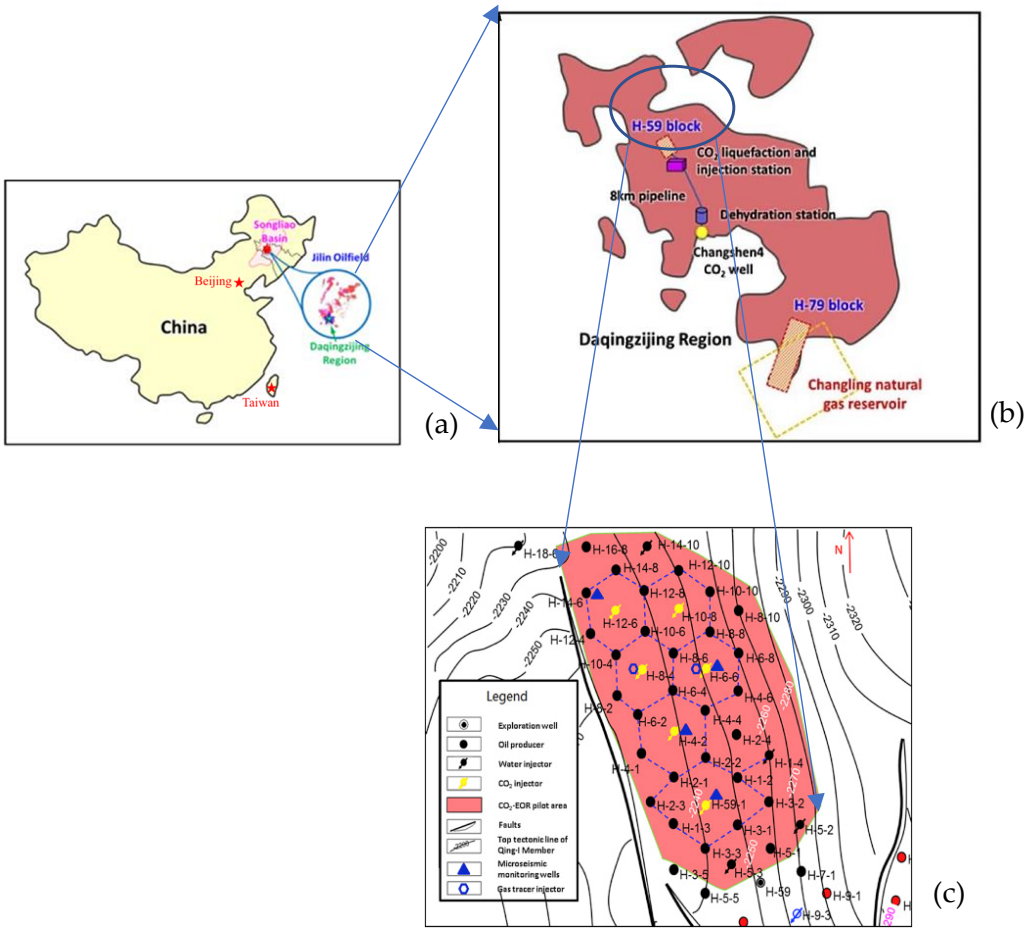

Figure 1. (**a**) Location of Jilin Oilfield (124.8° E, 45.1° N) [29]. (**b**) Main exploration areas [29]. (**c**) Site exploration well deployment map [30].

The regional exploration work of Daqingzijing block started in the early 1950s. At this stage, the basic geological structure of the area was mostly surveyed and understood

through the technical methods of physical exploration (the electric method, the magnetic method, gravity, etc.) [31].

In 2001, exploration work was completed in a total area of 600 km^2 in Daqingzijing block, and 3D seismic data within the area were collected and processed, and the block was officially entering the development stage. In several consecutive years, namely from 2000 to 2008, production was increased and the degree of reserve utilization in Daqingzijing block area exceeded 60%, with more than 1500 wells put into operation. The annual crude oil production was 100 × 10^4 t as a result of the decent development of the oilfield [32]. Figure 2 shows the composition of the crude oil production of Daqingzijing block over the mentioned years.

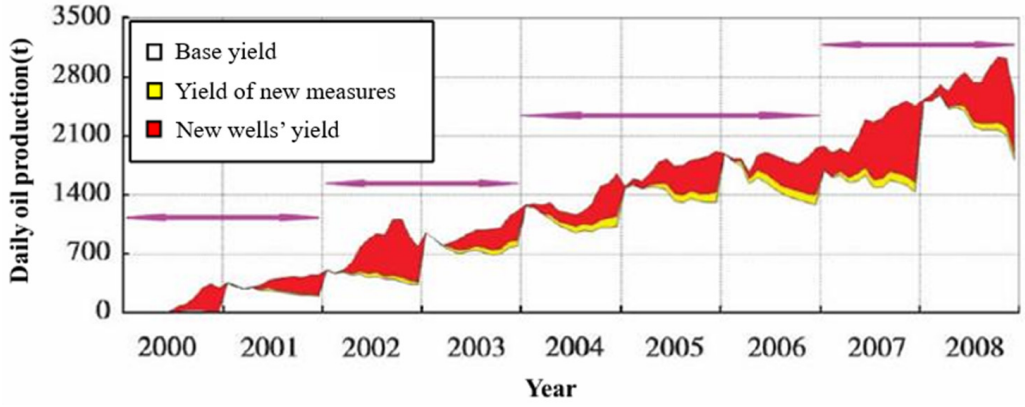

Figure 2. Historical crude oil production composition curve of Daqingzijing block [32].

At the end of 2010, Jilin Oilfield selected a total of 11 blocks such as Hei 79 and Hei 46 to promote the industrialization of CO2-EOR based on a series of achievements in theoretical research as well as indoor tests. A total of 171 gas injection wells and 697 oil production wells have been set up for oil recovery using the inverted five-point method.

Daqingzijing block is an early industrialized CO_2 flooding application oilfield in China, which has not only achieved an enhanced oil flooding operation but has also worked out a mature technology route and corresponding implementation measures through independent innovation. It provides a very valuable experience for the exploration of CO_2 flooding [33]. Therefore, Daqingzijing block seems to be very appropriate for the current study.

3. Theory and Equations

3.1. Three-Phase Relative Permeability

The existence of three-phase conditions in reservoirs requires the ability to approximate three-phase relative permeability. Various three-phase relative permeability models are implemented in TOGA (TOUGH Oil, Gas, Aqueous). Some are just simple extensions of two-phase (gas and water) relative permeability functions inherited from the TOUGH2 code (e.g., taking the "gas" relative permeability as a non-aqueous-phase relative permeability and then splitting it by the relative saturation of the gas phase in the non-aqueous phase).

The other functions are defined explicitly for three-phase conditions. In the following, we briefly describe the relative permeability models implemented in TOGA. The STONE II (IRP = 15) model assumes that the oil relative permeability can be estimated from the tabular data of the relative permeabilities of water–oil and oil–gas systems.

3.2. STONE II Model

When gas-, water-, and oil-phase conditions exist in a reservoir, the relative permeability is calculated by applying the modified STONE II model [34,35], which assumes that the relative permeability of the oil phase is a function of the relative permeability data of the

water–oil and oil–gas systems. The relative permeability data of these two systems need to be given by the user.

$$k_{ro}(S_l, S_g) = k_{rocl}\left[\left(\frac{k_{rol}}{k_{rocl}} + k_{rl}\right)\left(\frac{k_{rog}}{k_{rocl}} + k_{rg}\right) - (k_{rl} + k_{rg})\right] \quad (1)$$

where k_{rocl} is the relative permeability of the oil phase at a residual water saturation (S_{lc}), k_{rol} is the relative permeability of the oil phase at $S_g = 0$, and k_{rl} is the relative permeability function of the water phase in the water–oil system at an S_l saturation. k_{rog} is the oil-phase relative permeability associated with S_g when $S_l = S_{lc}$, and k_{rg} is the gas-phase relative permeability function associated with S_g in the gas–oil system. All two-phase relative permeabilities can be obtained by interpolating the tabular data by the smooth monotonic interpolation method proposed by Steffen [36] based on user-given data.

In TOGA, the water saturation could become smaller than the connate water saturation because the water could vaporize or be dissolved into oil and be carried away by the flowing gas–oil phase that would cause the local dry-out of the formation. In this case (i.e., $S_l < S_{lc}$), if the specified oil relative permeability k_{rocl} is less than 1, the two-phase relative permeabilities will be adjusted before using Equation (1) to calculate the oil relative permeability as follows:

$$k_{rog}^{new} = k_{rog}^{old} + \left(1 - k_{rocl}^{old}\right)\left(1 - \frac{S_l}{S_{lc}}\right)$$

$$k_{rg}^{new} = k_{rg}^{old} + \left(1 - k_{rgcw}^{old}\right)\left(1 - \frac{S_l}{S_{lc}}\right)$$

$$k_{rol}^{new} = k_{rol}^{old} + \left(1 - k_{rocl}^{old}\right)\left(1 - \frac{S_l}{S_{lc}}\right)$$

$$k_{rocl}^{new} = k_{rocl}^{old} + \left(1 - k_{rocl}^{old}\right)\left(1 - \frac{S_l}{S_{lc}}\right)$$

where superscript "*old*" indicates the values originally obtained from the interpolation of the tabular data whereas "*new*" indicates the adjusted value.

4. Model Setting

4.1. Simulator Introduction

TOGA is a numerical reservoir simulator for modeling the non-isothermal flow and transport of water, CO_2, multicomponent oil, and related gas components for applications including CO_2-EOR and geologic carbon sequestration in depleted oil and gas reservoirs. TOGA uses an approach based on the Peng–Robinson equation of state (PR-EOS) to calculate the thermophysical properties of the gas and oil phases, including the gas–oil components dissolved in the aqueous phase, and uses a mixing model to estimate the thermophysical properties of the aqueous phase.

TOGA uses a multiphase version of Darcy's Law to model the flow and transport of mixtures through porous media with up to three phases over a range of pressures and temperatures appropriate for hydrocarbon recovery and geologic carbon sequestration systems. The transport of the gaseous and dissolved components is assumed to be taking place by advection and Fickian molecular diffusion. New methods for phase partitioning and thermophysical property modeling in TOGA have been validated against experimental data published in the literature for describing phase partitioning and phase behavior. Flow and transport had been verified by testing against related TOUGH2 EOS modules and CMG (Computer Modelling Group) simulators [37].

The TOGA simulator adopts the integral finite difference method for spatial discretization. For time discretization, it employs the fully implicit differences with unconditional convergence.

4.2. Geomodel and Boundary Conditions

The selected simulation area was the Jilin Oilfield Daqingzijing block. The actual reservoir conditions were used as the basis of the numerical simulation to construct the three-dimensional numerical model of the reservoir in the study area. A relatively complete five-point well network for the injection and production area was selected as the modeling domain. The boundary and the geological conditions of the reservoir were set as the confining boundary to simplify the simulation.

The reservoir in the area can be categorized as a stratified, low-permeability sandstone reservoir. To simplify the model, the reservoir was generalized as a low-permeability sandstone reservoir with horizontal stratification and a homogenous thickness, without considering its fracture development. The thickness of the reservoir was set to 10 m. The upper and lower caprocks of the reservoir were simplified as no-flow boundaries.

According to the actual situation of the oilfield, a 140 m × 140 m, five-point-method well network was used for injection and extraction. As shown in Figure 3, the pink square is the research area used to construct the conceptual model. One injection well (red circle in Figure 3) and one production well (blue circle) were considered at both ends of the square diagonal. CO_2 was injected through the injection well at a fixed rate. The fluid was extracted from the production well at a given pressure. Due to the symmetric properties of the five-point well network, the boundaries around the research area could be simplified as no-flow condition types.

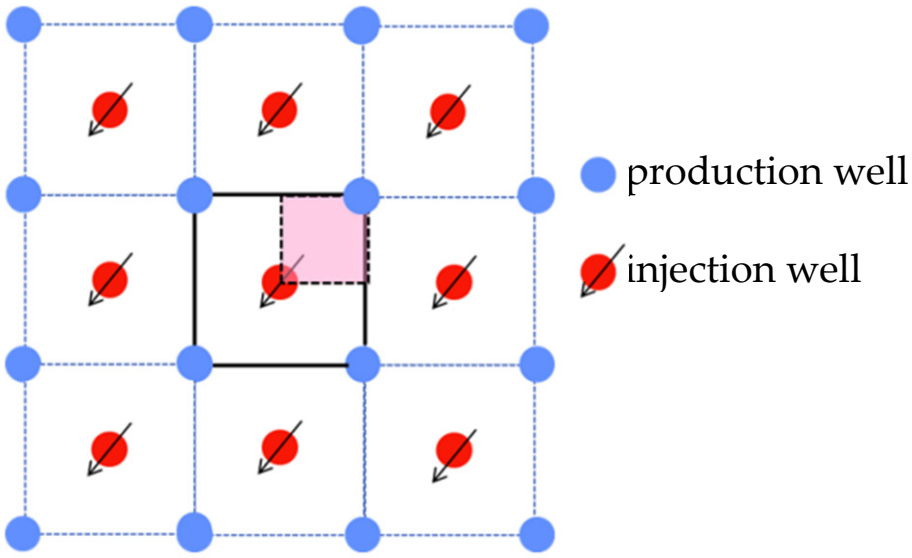

Figure 3. Schematic of the five-point well network and modeling area.

To simplify the modeling, the anisotropy in the reservoir properties was ignored and the model was assumed to be isotropic and homogeneous, with a small thickness. The three-dimensional simulation model was dissected in the horizontal plane into 14 × 14 segments with a total of 196 grids and was vertically divided into five layers with a total of 980 grids.

The entire model was a rectangular cube with a length of 140 m, a width of 140 m, and a height of 50 m. Each cell was also a cube of 10 m in length, 10 m in width, and 10 m in height. The grid dissection is shown in Figure 4. The bottom cell on the left side of the figure was selected as an injection well for constant-rate CO_2 injection, while the bottom cell on the right side was assumed to be a production well. Additionally, the yellow color in Figure 4 is the injection–production profile of the reservoir.

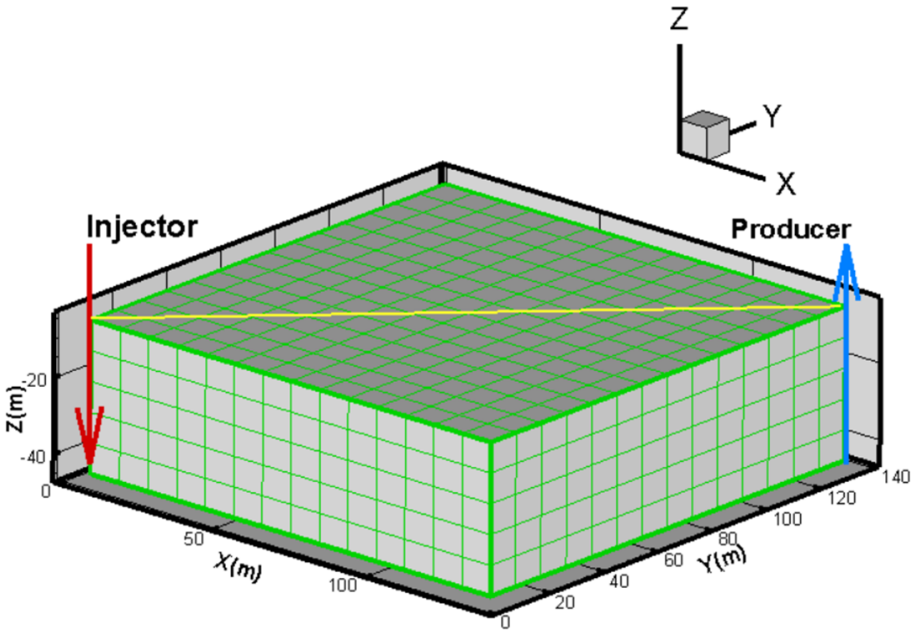

Figure 4. Reservoir sectional grid map.

4.3. Thermo-Hydrological Parameters and Initial Conditions

4.3.1. Thermo-Hydrological Parameters

Based on the data summarized from previous studies and the relevant information from Jilin Oilfield, the average values of the initial physical properties of the reservoir in the study area are presented in Table 1.

Table 1. Thermo-hydrological parameters [29,30,38].

Parameter	Value	Parameter	Value
temperature (°C)	98.9	MMP (MPa)	22.3
average porosity (%)	12.7	reservoir fracture pressure (MPa)	49
average permeability (mD)	3.0	oil viscosity (mPa.s)	2.02
initial well-head pressure (MPa)	24.15	oil density (g/m^3)	0.765
reservoir thickness (m)	11.2–18.2	oil saturation (before CO_2 injection)	0.35–0.38
salinity (ppm)	14,607		

4.3.2. Initial Conditions

Stratigraphic crude oil is a complex mixture of various hydrocarbon and non-hydrocarbon compounds. It is difficult to determine and quantify the physical and chemical properties of each component of crude oil, so it is necessary to construct the components of crude oil by using curve fitting and mathematical modeling based on the physical characteristics of crude oil presented elsewhere [39]. The initially proposed crude oil components of this study were obtained from previous studies, and their specific parameters are presented in Table 2.

Table 2. Properties of crude oil [30].

Components	CO_2	N_2 to Cl	C2 to C6	C7+
mole fraction (%)	0.407	15.574	24.384	59.635
critical pressure (atm)	72.8	44.2	41.24	15.35
critical temperature (°C)	30.42	18.35	38.71	73.54
critical volume (cm^3/mol)	94	97.89	21.45	87.69
molar mass (g/mol)	44.01	17.3	48.88	24.56
acentric factor	0.225	0.013638	0.16345	0.34353

The relative permeabilities of gasses, oil, and aqueous phases are important during CO_2 flooding within a reservoir. The STONE II model is commonly employed to calculate these relative permeabilities [40]. To obtain the proper parameters of the STONE II model, the regression technique was used based on the relative permeability curves (Figure 5) from Zhang et al. [29]. The relevant parameter settings in the STONE II model are summarized in Table 3.

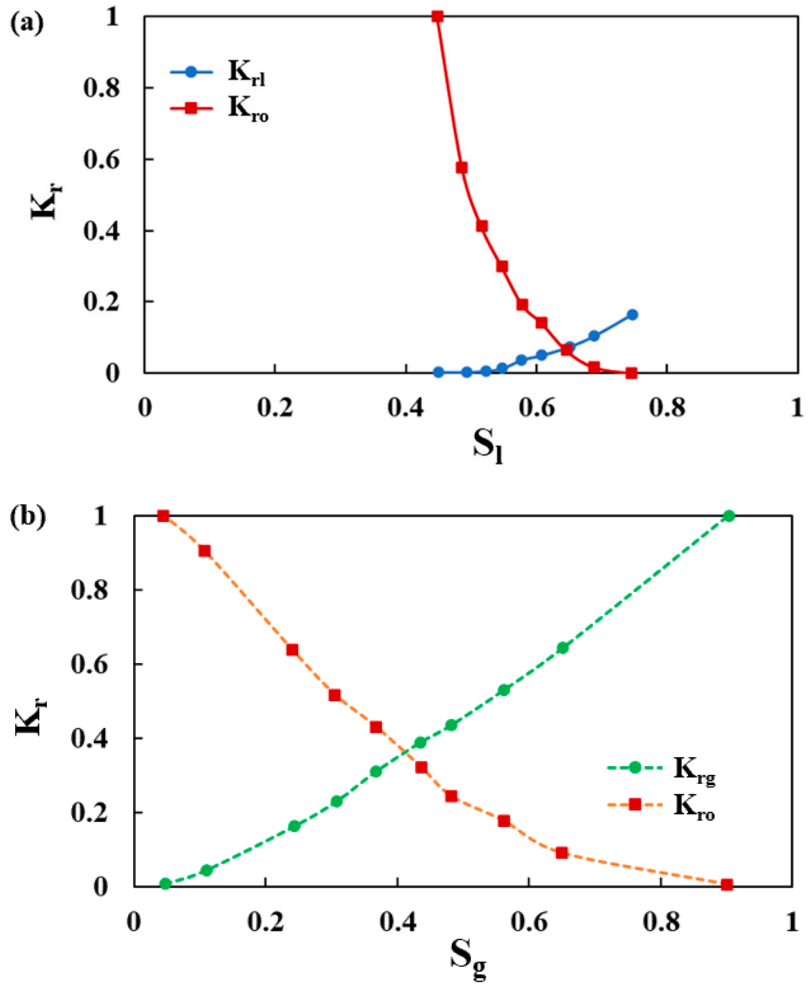

Figure 5. (**a**) Water–oil relative permeability curve; (**b**) gas–oil relative permeability curve [29].

Table 3. Parameter settings for STONE II model.

Parameter	Value
S_{lc}: Residual water saturation	0.45
S_{gc}: Residual gas saturation	0.05
k_{rol}: When $S_g = S_{lg}$, relativeoil − phase permeability with respect to S_l.	Figure 5a
k_{rl}: When $S_g = S_{lg}$, relativeliquid − phase permeability with respect to S_l.	
k_{rocl}: When $S_l = S_{lc}$, relative oil-phase permeability.	1.0
k_{rog}: When $S_l = S_{lc}$, relative oil − phase permeability related to S_g.	Figure 5b
k_{rg}: When $S_l = S_{lc}$, relative gas − phase permeability related to S_g.	

4.4. Case Design

To achieve these objectives, we generated random heterogeneous fields of hydrological parameters [41] (permeability and porosity). In this study, three kinds of reservoir characteristics were set up: homogeneous formation, layered heterogeneous formation, and

spatially heterogeneous formation. By specifying the same initial conditions, gas injection volume, and oil flooding time, comparative analysis was carried out to obtain the influence of the heterogeneities of the hydrological parameters on the oil recovery of CO_2 flooding.

4.4.1. Homogeneous Formation

Based on the thermo-hydrological parameters in Section 4.3.1, some parameters were optimized to model the reservoir. The permeability and porosity of the reservoir were unchanged, the simulation time was set to 20 years, and carbon dioxide was injected at a constant rate of 1.5625×10^{-3} kg/s. The pressure of the production well was considered 18 MPa.

4.4.2. Layered Heterogenous Strata

The oil reservoirs in Jilin Oilfield are distributed in different strata, and the bottom strata consist of alternating layers of mudstone and sandstone with different permeabilities and porosities.

As a result, the layered heterogenous strata model set up mudstone and sandstone with different permeabilities to be interbedded in the vertical direction (five layers in total) and in the horizontal direction. The permeability of the reservoir was considered constant. The rest of the parameters were assumed to be the same as the homogeneous model.

Due to the lack of actual data from Jilin Oilfield, the average value of the porosity of the reservoir in the study area was moved up and down by 40%, and the order of magnitude of the permeability was adjusted up and down by two orders of magnitude to form the high-permeability and low-permeability layers. The specific data are shown in Table 4, and the reservoir was set up as an interbedded layer of siltstone–mudstone–siltstone–siltstone–mudstone–siltstone. Figure 6 shows the final effect of the layered heterogenous reservoir model setup.

Table 4. Layered heterogenous model reservoir parameters.

Permeability	Rock Type	Permeability m^2	Porosity %
High	Siltstone	2.961×10^{-13}	17.78
Low	Mudstone	2.961×10^{-17}	7.62

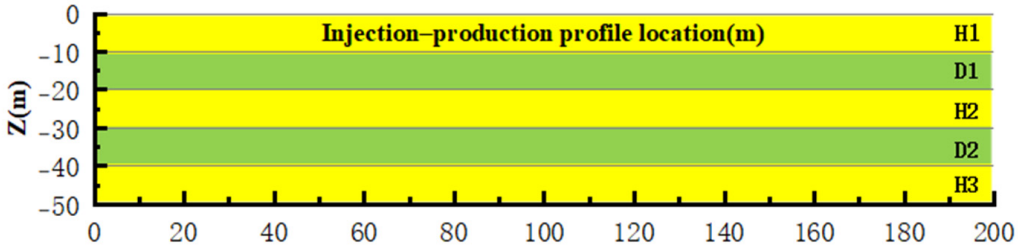

Figure 6. Layered heterogenous reservoir model (H: high permeability; D: low permeability).

4.4.3. Spatially Heterogenous Strata

The construction of the spatially heterogenous model used the random field theory detailed by Vanmarcke and Grigoriu [42]. According to the data from Jilin Oilfield, to obtain the spatial distribution of the reservoir permeability and porosity, the permeability was taken as an average value according to the overall normal distribution and was also randomly distributed in different grids (porosity was positively correlated with permeability). Figure 7 displays the spatial distribution of the reservoir porosity.

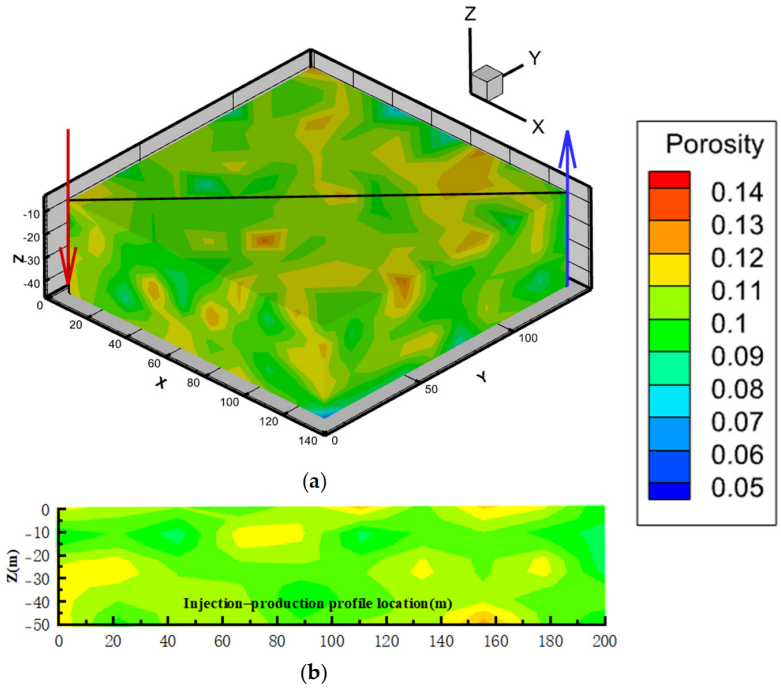

Figure 7. Spatial heterogeneity: (**a**) spatial distribution of reservoir porosity; (**b**) porosity distribution of reservoir injection–production profile.

5. Results and Discussion

5.1. Influence of Heterogeneity on Distribution of Residual Oil Phase in Reservoirs

The initial oil saturation of the three models is shown in Figure 8, which is the same as 0.37. The red color in Figure 8 is the injection well and the blue color is the production well. The yellow color is the location of the dissection of the injection–production profile. The effect of heterogeneity on the distribution of the residual oil phase in the reservoir is observed through the variation in oil saturation.

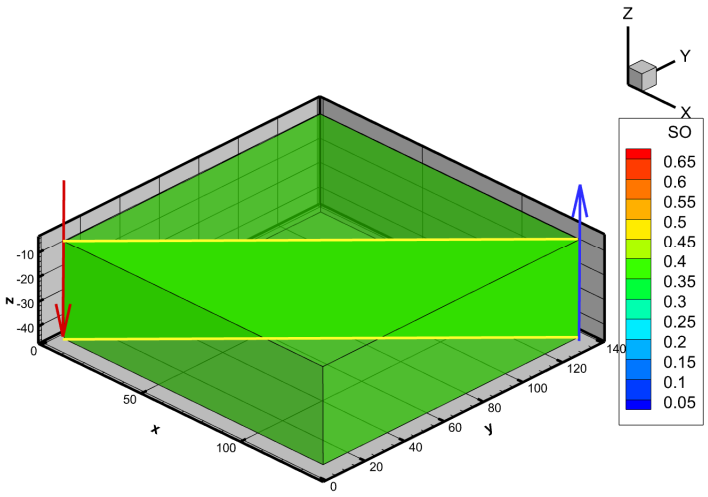

Figure 8. Spatial distribution of initial oil saturation of homogeneous model.

To facilitate the observation, the oil saturation variations in the injection–production profiles are analyzed. The distribution of the oil saturation (in the injection–production profiles) through different years of production in the homogeneous model is presented in Figure 9.

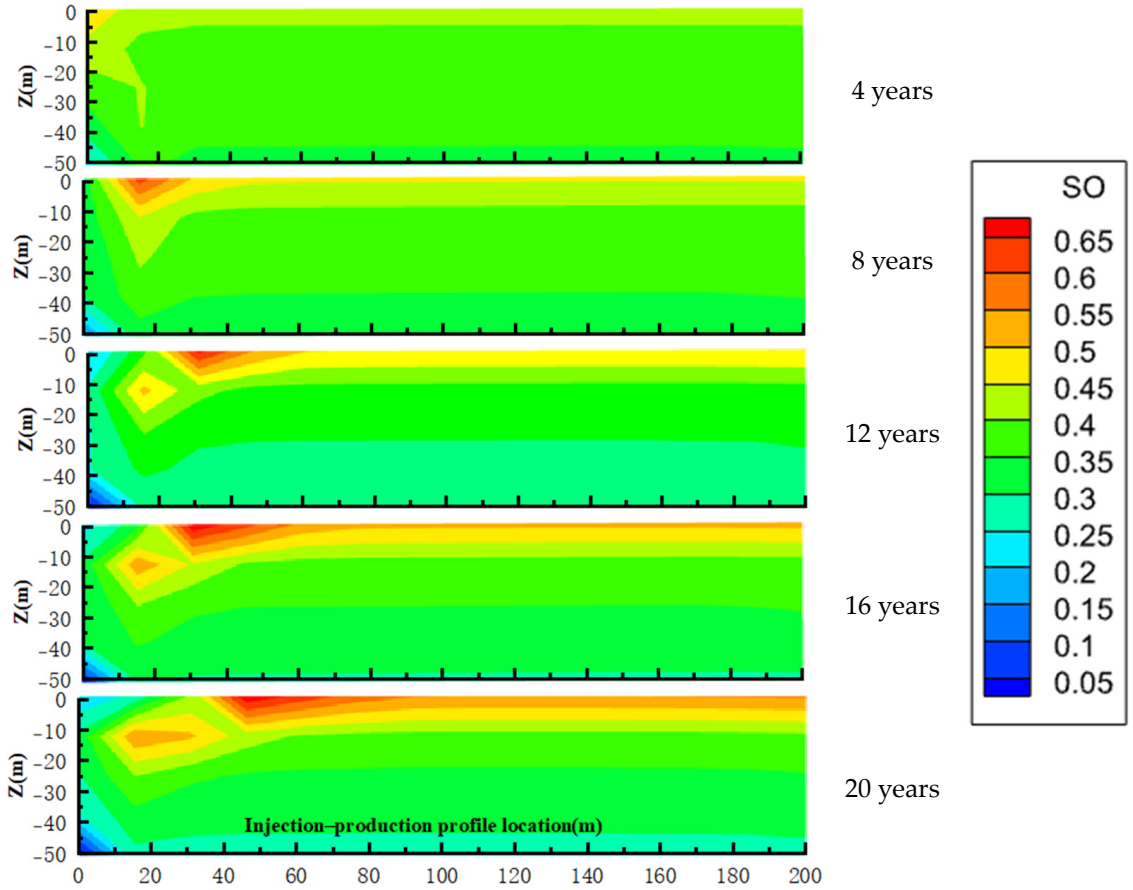

Figure 9. Oil saturation in the injection–production profile of the homogeneous model.

As can be observed from the figure, in general, the oil saturation changes in the homogeneous model mainly occurred at the top of the reservoir and near the injection wells. With the injection of CO_2, the oil phase in the reservoir gradually accumulated and formed areas with high oil saturation (oil saturation greater than 0.55), and these highly saturated areas of the oil phase gradually moved toward the production well. Consequently, there was a trend of oil-phase replacement in the reservoir from the injection wells towards the production wells. Spatially, the highest oil saturation of the reservoir was 0.65. At the injection well, the oil saturation of the reservoir decreased significantly. Moreover, the oil phase of the reservoir gathered in the upper reservoir near the injection well. There were two obvious centers of high oil saturation (oil saturation greater than 0.55), which signified the phenomenon of the uplift of the oil phase in the homogeneous model. This oil-phase uplift led to the phenomenon of the layering of the oil saturation, in which the oil saturation in the upper reservoir was higher than that in the bottom. Therefore, the oil flooding effect was more obvious in the upper part of the reservoir.

In general, the starting point of CO_2 flooding was from the bottom. This allowed the oil phase to gather at the top of the reservoir under the action of buoyancy and CO_2 flooding. The displacement speed was faster in the vertical direction and slower in the lateral direction. Therefore, the oil accumulated at the top of the reservoir and moved with the CO_2 flooding, forming two oil-phase accumulation zones. Because of the different times of formation, the two oil accumulation areas were not continuous. In the process of oil recovery in the actual site, there would also be a slight oil-phase floating phenomenon because the thickness of the reservoir is thick, so the oil-phase uplift phenomenon would be more obvious.

Figure 10 displays the distribution of oil saturation in the injection–production profiles for different years of production for the layered heterogenous model.

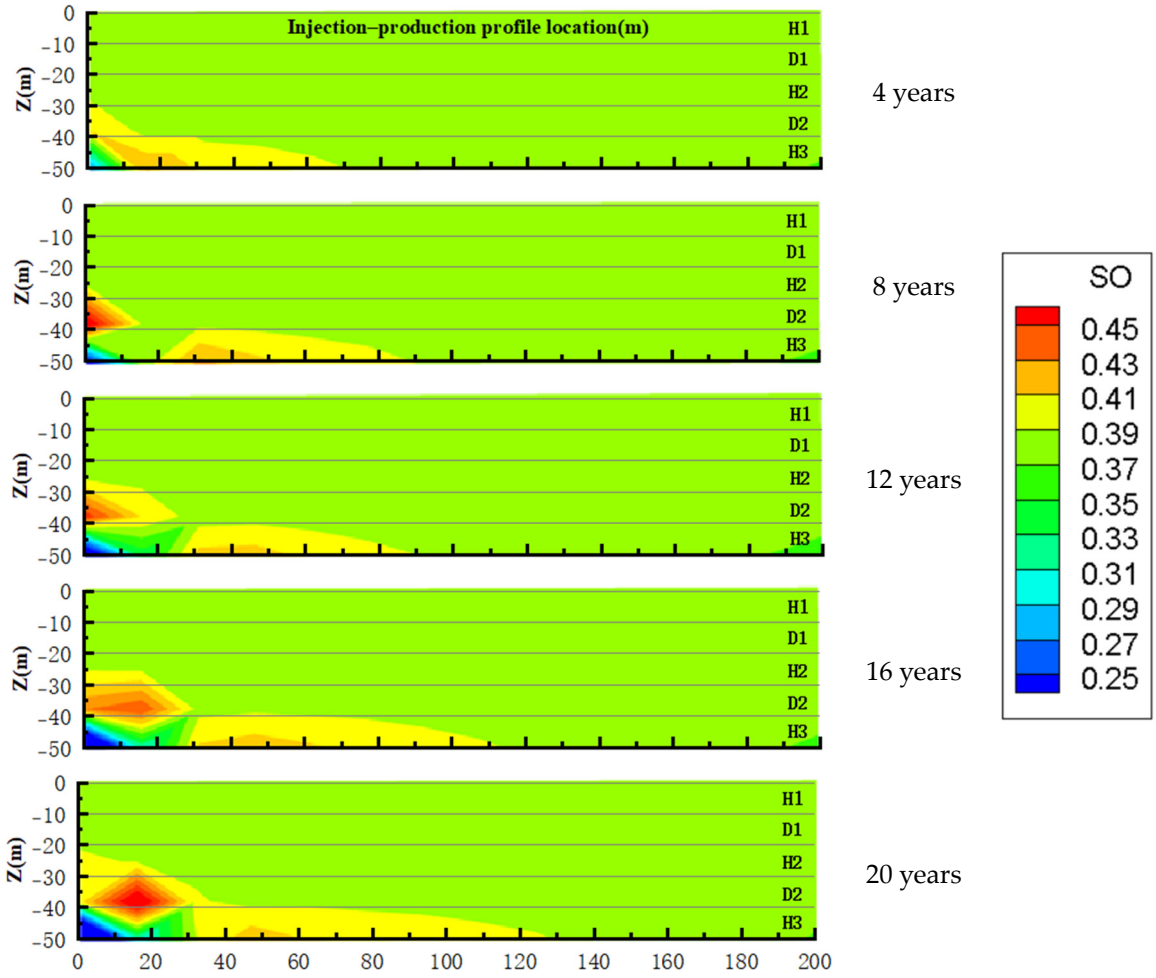

Figure 10. Oil saturation in the injection–production profile of the layered heterogenous model.

Laterally, due to CO_2 injection, the oil phase in the reservoir was gradually transported towards the production well. It could be found that the oil phase in the H3 (specified in Figure 6) reservoir had a very good flooding effect, and in the part near the injection well, the oil saturation was reduced, and the area with high oil saturation had been transported to two-thirds of the injection–production profile. Vertically, due to the existence of the low-permeability reservoir, D2, the CO_2 could not be smoothly transported from the bottom of the reservoir to the top. This caused the CO_2 to recover the oil, which was present in only two layers in the model (layers D2 and H3). The oil-repelling effect of the D2 layer was poor, and a large amount of oil was accumulated in the left side of the D2 layer, and the transportation speed to the production wells was very slow. The difference in the repelling effect caused the difference in the spatial distribution of the oil saturation, and, hence, there was a situation of intermittent, discontinuous oil saturation.

Generally speaking, the oil flooding effect of the layered heterogenous model was more obvious in the lower layer of the reservoir, in which the oil phase was mainly concentrated in the bottom of the reservoir, and only the oil saturation of the D2 and H3 layers changed significantly. The transport of the oil saturation of the layered heterogenous model had the characteristics of oil production by layer, distinguishing the transport of different reservoirs. Comparing the D2 and H3 layers, there was a center of higher oil saturation in both reservoirs, which showed the displacement of the two reservoirs, respectively.

Comparing the reservoir settings of the layered heterogenous model in Section 4.4.3, it can be concluded that the lowest reservoir (H3) was a highly permeable reservoir, while D2 was a low-permeability reservoir, which indicates that the injected CO_2 preferentially flooded off the oil in the reservoir with better permeability.

In addition, there was no oil-phase stratification in the reservoirs of the layered heterogenous model, which may have been due to the low-permeability strata in the layered inhomogeneous strata hindering the vertical transportation of the oil phase.

Figure 11 displays the spatial distribution of oil saturation for the spatially heterogenous model. Temporally, the oil saturation in the part of the reservoir close to the injection wells decreased continuously with the CO_2 injection. The oil saturation in the injection wells was about 0.25 after 4 years of simulation, and most of the areas with a saturation of 0.15 or less were already present after 12 years. The oil saturation in the areas with good reservoir permeability gradually increased with the CO_2 injection. After 4 years, the oil saturation in the areas with good permeability was about 0.5, whereas after 20 years, the oil saturation in these areas had already reached 0.75, with an increase in the number and extent of these areas.

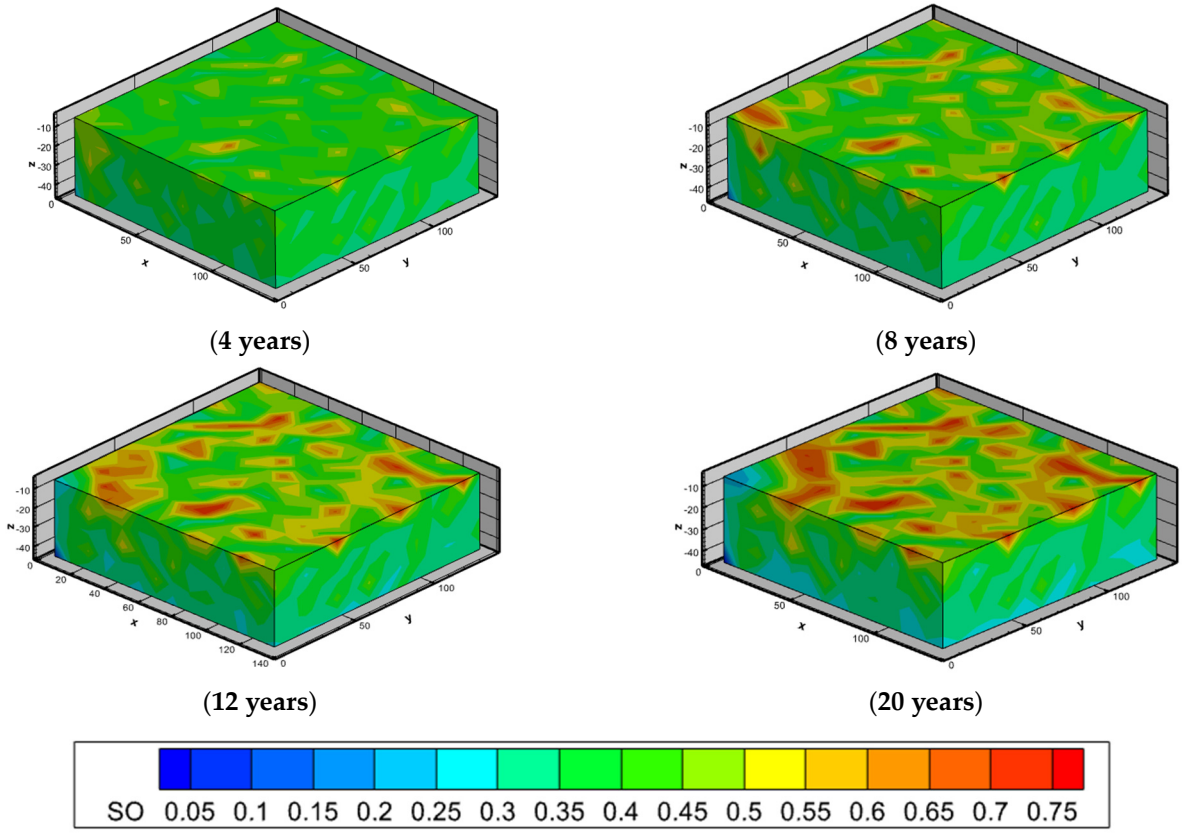

Figure 11. Oil saturation for spatially heterogenous modeling of spatial distribution.

Spatially, the areas with higher oil saturation tended to be transported to the production wells, and the reservoir also showed the phenomenon of oil-phase uplift.

To further understand the effect of the spatial non-uniform distribution of permeability and porosity on the distribution of the remaining oil phase, the spatially heterogenous model's oil saturation injection–production profile distribution is plotted in Figure 12.

Comparing Figures 6 and 7, it can be found that the high-oil-saturation area of the reservoir corresponded to the area with high permeability and high porosity, which indicates that the spatially heterogenous model of the displacement contained the two characteristics of the homogeneous model and the heterogenous model of the displacement. Unlike the stratified heterogenous model, due to the uneven distribution of permeability and porosity in the reservoir, the oil phase in the reservoir could only be connected to the adjacent high-permeability reservoir to realize the transportation, and because of the uplift of the oil phase similar to that of the homogeneous model, these uplifted oil phases, flooded by CO_2, would gather at the top of the reservoir to choose the area with better permeability and move to the production wells.

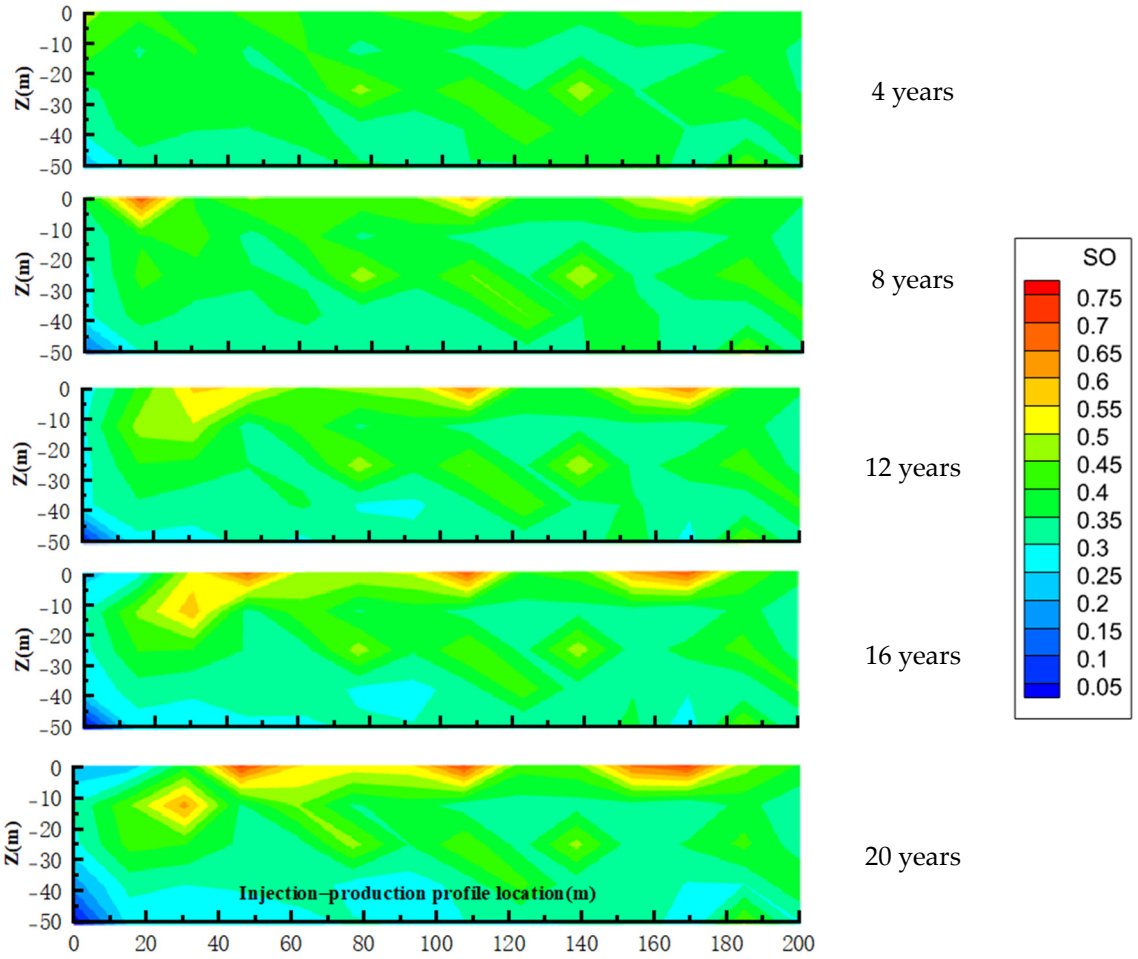

Figure 12. Oil saturation in the injection–production profile of the spatially heterogenous model.

5.2. Influence of Heterogeneity on CO_2 Distribution in Reservoirs

The oil production of the reservoir can be better analyzed by examining the transport of CO_2 in the reservoir. In this section, the CO_2 gas saturation distribution maps of the reservoir are explored for comparative analysis. The gas saturation injection and production profile distribution maps of the three different reservoirs (homogeneous, layered heterogenous, and spatially heterogenous) in different years are plotted in Figure 13. As observed in Figure 13, the injected CO_2 is all concentrated in one-third of the reservoir's injection-well side.

Based on Figure 13 a, the CO_2 was injected from the bottom of the reservoir, was gradually transported upward, and finally (after 20 years) began to diffuse at the top of the reservoir.

Observing the gas saturation distribution of the injection–production profile of the layered heterogenous model (Figure 13 b), after CO_2 injection, the CO_2 did not move to the upper part of the reservoir as it did in the homogeneous model but moved along the bottom of the reservoir towards the production wells. This was due to the fact that the bottom part of the reservoir was highly permeable with high porosity, while the lower permeability of the reservoir in the middle part restricted the upward CO_2 movement. This, in turn, made the majority of CO_2 enter the high-permeability part of the reservoir at the bottom, and, thus, the oil-phase replacement of the reservoir mainly occurred in the lower part of the reservoir.

Figure 13c displays the gas saturation along the injection–production profile for the spatially heterogenous model, which indicates that the gas saturation distribution of the spatially heterogenous model was similar to that of the homogeneous model. The CO_2 was

injected from the bottom of the reservoir and gradually transported upward and finally started to diffuse at the top of the reservoir. This could be attributed to the fact that the spatially heterogenous model, because of the random porosity–permeability condition, did not form a relatively closed low-permeability capping layer like that of the layered heterogenous model. This, in turn, allowed the upward transport of the injected CO_2 in the reservoir.

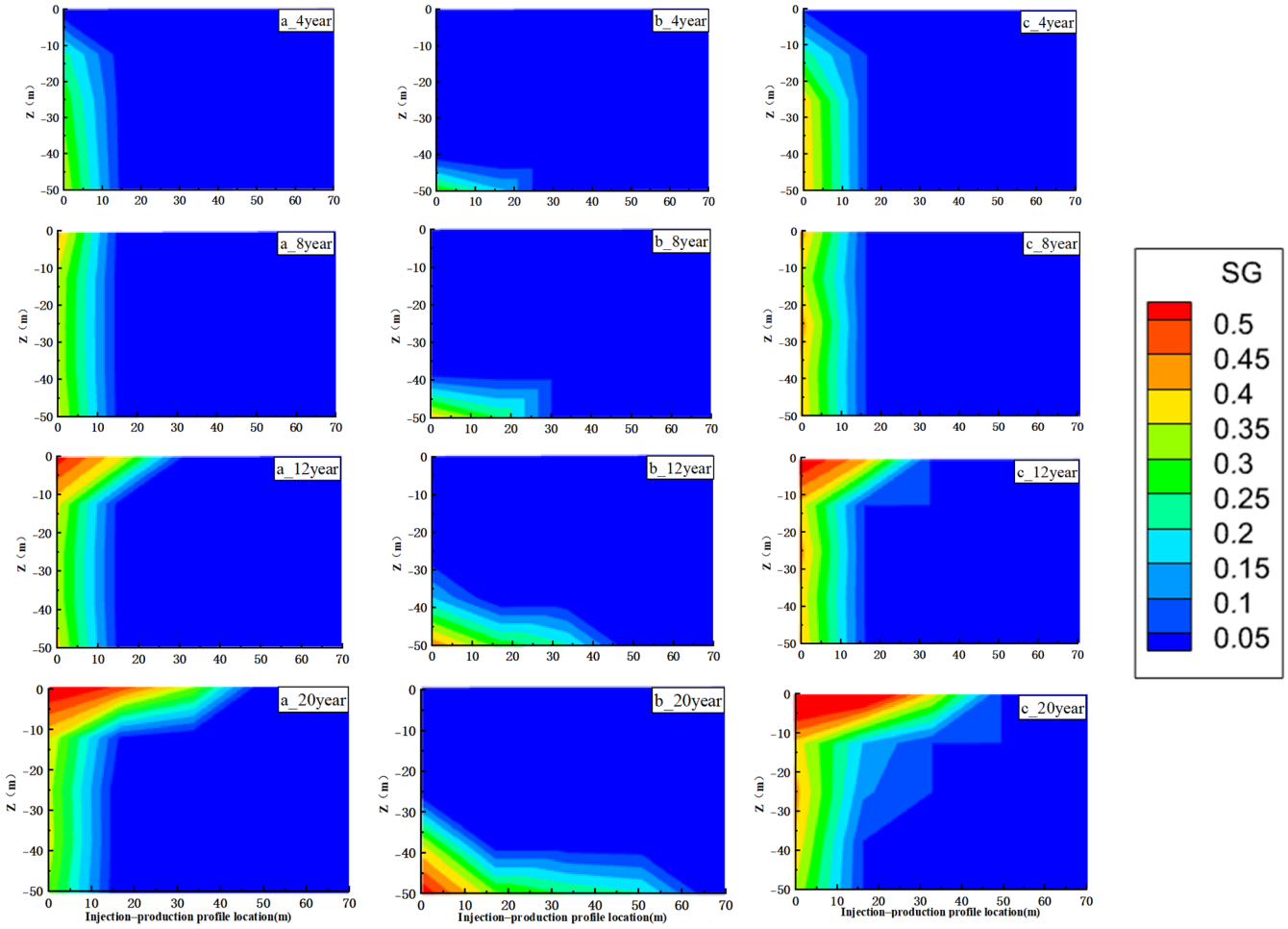

Figure 13. Distribution of gas saturation along injection–production profiles (on injection-well side): (**a**) homogeneous model; (**b**) layered heterogenous model; (**c**) spatially heterogenous model.

The difference between the gas saturation distribution maps of the spatially heterogenous model and the homogeneous model is that the CO_2 in the homogeneous model was uniformly diffused upward while the upward diffusion of the CO_2 in the spatially heterogenous model was uneven, as can be observed from Figure 13. The areas with high gas saturation close to the side of the injected wells were not contiguous but rather were in the form of a jagged distribution. Moreover, the injected CO_2 in the spatially heterogenous model was transported laterally in addition to the upward transport (Figure 13 c_20 years). According to Figure 7, these regions had higher permeability, which indicates that the injected CO_2 would preferentially diffuse into regions with higher permeability in the process of CO_2-EOR.

5.3. Influence of Heterogeneity on Cumulative Oil Production

Figure 14 presents the cumulative water, CO_2, and oil production from different years of the simulation. The cumulative production of the CO_2 from the production well after 20 years of simulation in the homogeneous model was 8.11×10^2 kg, while the cumulative water production was 2.46×10^6 kg, and the cumulative output of the oil phase

was 1.51 × 10^4 kg. After continuous injection, the quantity of the water phase from the production well was much higher than that of the CO_2 and oil phases, which was probably due to the fact that the initial water content was high, and during the CO_2 injection, these water phases were flooded out of the reservoir along with the oil phase. The CO_2 had the lowest production amount, which may have been due to the fact that the injected CO_2 had not yet been transported to the production well and all the CO_2 output at this stage was the CO_2 initially contained within the reservoir.

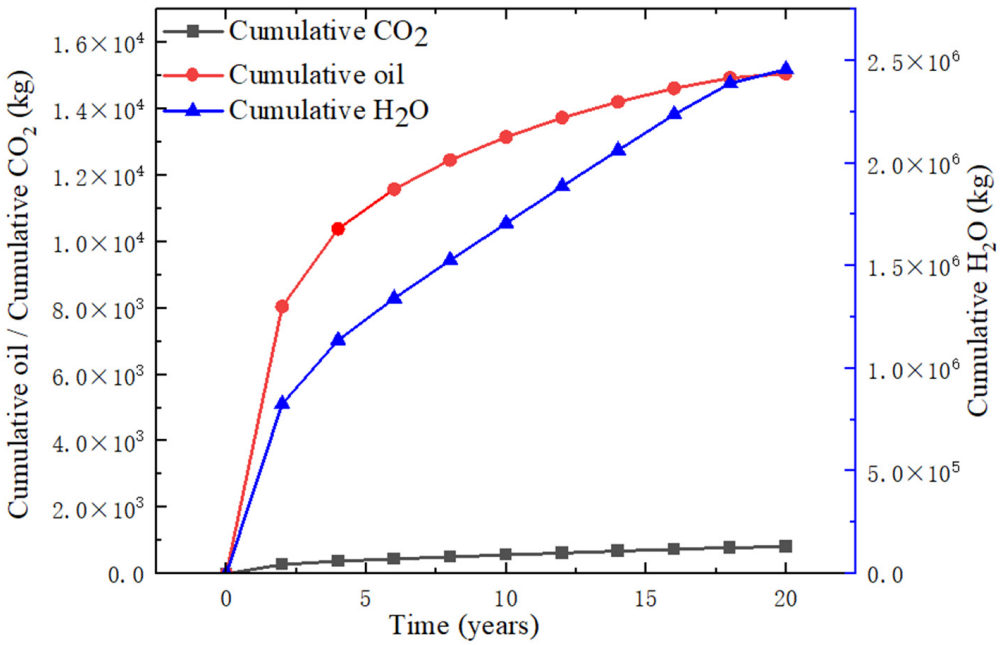

Figure 14. The cumulative amount of each phase in the production well for the homogeneous model.

In addition, with the injection of CO_2, the rate of oil production gradually decreased and the amount of oil production gradually tended to stabilize.

The cumulative production of the CO_2 phase after 20 years from the production well in the layered heterogenous model was 9.57 × 10^2 kg, the cumulative output of the water was 2.66 × 10^6 kg, and the cumulative output of the oil was 8.46 × 10^4 kg. The cumulative productions at different years of the simulation are plotted in Figure 15.

With the injection of CO_2, the output efficiency of the water and oil phases of the reservoir was high in the beginning (after 2 years of production). However, the subsequent output efficiency decreased and remained low. The CO_2 output efficiency of the reservoir did not change significantly with time, which indicates that the injected CO_2 had not yet reached the output well, and gas flushing did not occur.

Compared to the homogeneous model, the layered heterogenous model was more effective in flooding oil as more oil was produced after 20 years of production.

The cumulative output of the CO_2 from the production well for the spatially heterogenous model after 20 years was 8.11 × 10^2 kg, the cumulative output of the water phase was 2.45 × 10^6 kg, and the cumulative output of the oil phase was 1.42 × 10^4 kg. The cumulative production of these phases at different years are plotted in Figure 16.

The production volumes of each phase of the spatially heterogenous model were basically very close to those of the homogeneous model. However, the output volume of the oil phase was slightly smaller than that of the homogeneous model. This was due to the existence of some randomly distributed low-permeability areas in the reservoir, which could affect the oil flooding effect of the CO_2 if they were distributed along the injection–production profile.

The cumulative production data from the three cases are summarized in Table 5.

Table 5. Comparison of cumulative production from different cases.

Case / Output (kg)	Injection	Production		
	All Three Models Are The Same	Homogeneous	Layered Heterogeneity	Spatial Heterogeneity
CO_2	9.856×10^5	8.11×10^2	9.57×10^2	8.11×10^2
Water	0	2.46×10^6	2.66×10^6	2.45×10^6
Oil	0	1.51×10^4	8.46×10^4	1.42×10^4

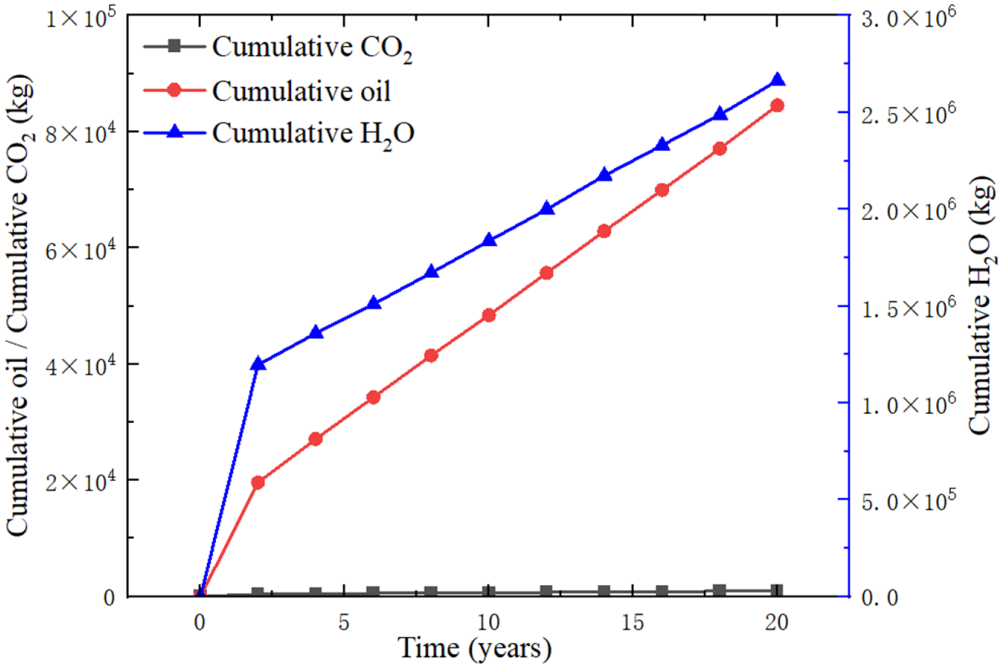

Figure 15. The cumulative amount of each phase in the production well for the layered heterogenous model.

Based on Table 5, it can be concluded that with the same amount of injected CO_2, the layered heterogenous model had the best oil displacement effect, with its oil displacement amount reaching 8.46×10^4 kg, while the homogeneous model and the spatially heterogenous model had lower values.

The year-by-year change in the oil recovery volume of different cases is plotted in Figure 17, which shows that with the injection of the gas phase, the cumulative oil phase output from each case continued to accumulate, among which the cumulative oil recovery volume of the layered heterogenous model was the largest, the cumulative oil recovery volume of the homogeneous model was the second largest, and the cumulative oil recovery volume of the spatially heterogenous model was the smallest.

The largest cumulative oil removal in the layered heterogenous model may have been due to the existence of a continuous hypertonic reservoir connecting the injection wells and the output wells in this model, where CO_2 could replace the oil phase more easily. Meanwhile, the homogeneous model and the spatially heterogenous model did not have such a connecting reservoir. The spatially heterogenous model may have had a low-permeability region in the reservoir, which may have made it difficult to transport CO_2 in the reservoir, thus affecting the oil removal efficiency of the reservoir, resulting in less oil removal in the spatially heterogenous model than in the homogeneous model.

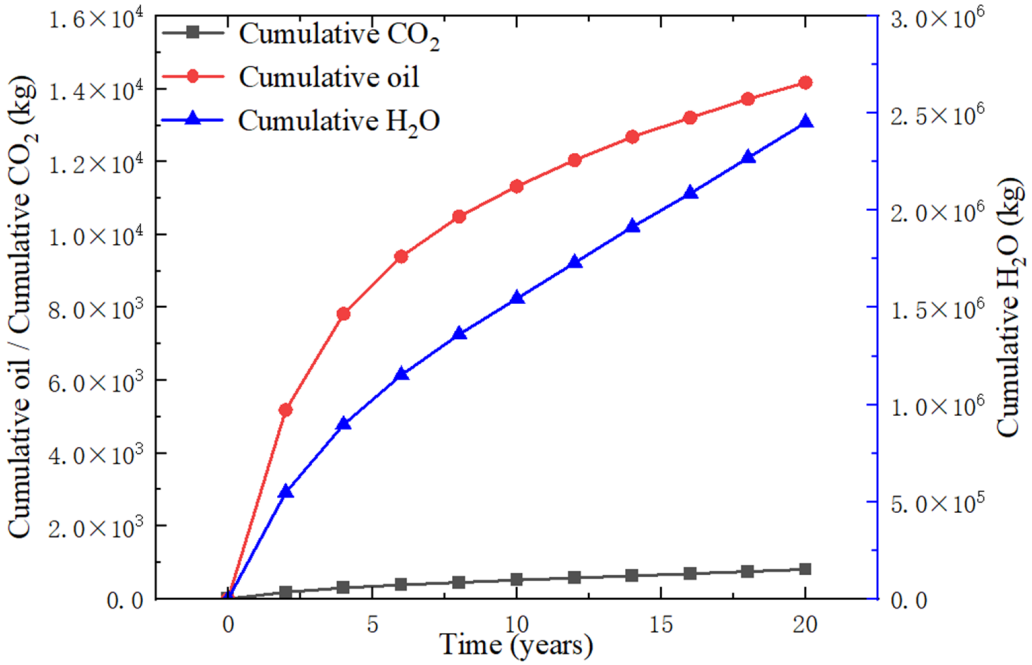

Figure 16. The cumulative amount of each phase in the production well for the spatially heterogenous model.

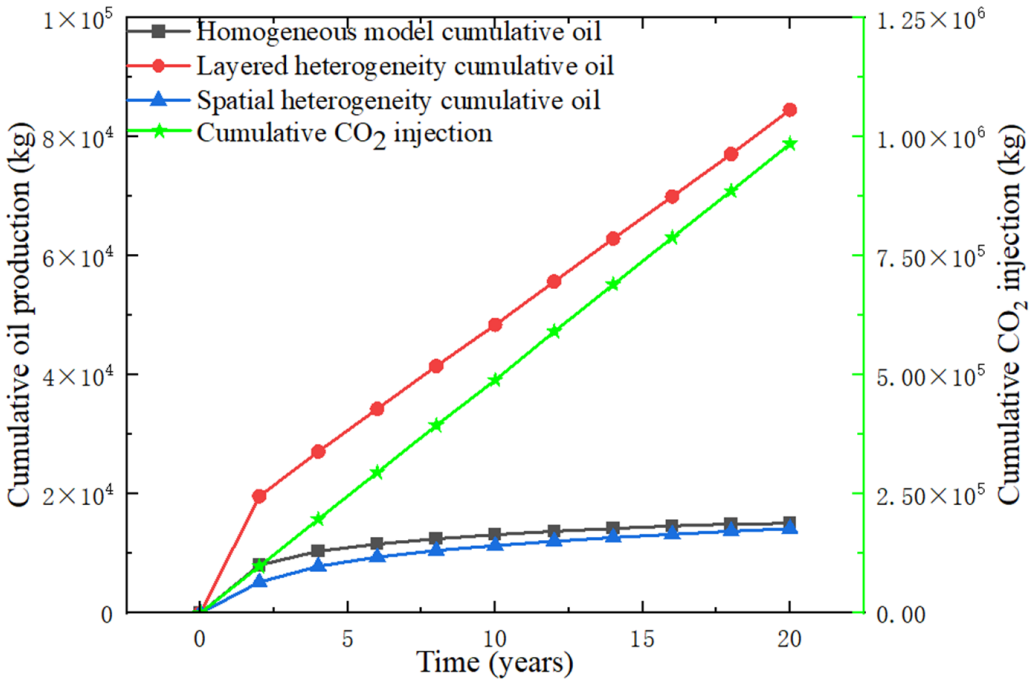

Figure 17. CO_2 injection volume and oil repelling volume of different cases.

6. Conclusions

In this work, three CO_2-EOR cases of oil reservoirs' conditions of permeability were set up. After the end of the flooding off, the distribution of the remaining oil phases as well as the distribution of the CO_2 in the reservoirs were analyzed to understand the characteristics of CO_2 flooding in different reservoir conditions. By changing only one property in each simulation case, and comparing the amount of oil production, the case with the best oil production effect was determined. The following conclusions can be made from this study:

(1) It can be concluded that, under the same injection volume condition, the cumulative oil flooding effect of the layered heterogenous model was the best, the cumulative oil flooding amount of the homogeneous model was the second best, and the spatially heterogenous model had the worst oil flooding effect.
(2) In different cases, high oil saturation centers would appear in the process of CO_2 flooding. They were generally formed near the injection wells and in the areas with good permeability. The centers of high oil saturation were formed for different reasons. With the injection of CO_2, these centers would gradually move to the production wells, and the location and movement of the high oil saturation corresponded to the modeled oil flooding effect.
(3) In the process of CO_2 flooding, if the porosity–permeability conditions of the reservoir were consistent, the oil phase had a tendency to float upward, which would cause the oil phase in the reservoir to float on the top of the reservoir, and then the oil at the top of the reservoir would be flooded off preferentially.
(4) In the process of CO_2 flooding, when the porosity and permeability of the reservoirs varied spatially, the flooding effect of the CO_2 in the highly permeable reservoirs was better than that in the low-permeability reservoirs. The transport of oil in the layered heterogenous model appeared to have different behaviors between layers. In the spatial heterogenous model, the oil phase flooded by the CO_2 gathered at the top of the reservoir and moved to the production wells through the zones with higher permeabilities.

Author Contributions: Conceptualization—Formal analysis and Software, Z.L. and H.T.; Data curation—Investigation and Methodology, Z.L. and R.P.; Funding acquisition—Project administration and Resources, T.X.; Validation—Visualization and Writing—Original draft, Z.L.; Supervision, T.X.; Writing—Review and editing, H.T. and T.X. All authors have read and agreed to the published version of the manuscript.

Funding: This work was performed in support of the National Natural Science Foundation of China (Grant No. 42141013) and Jilin Province Science and Technology Department Development Plan Project (Grant No. YDZJ202401330ZYTS).

Data Availability Statement: The data that support the findings of this study are available on request from the corresponding author.

Acknowledgments: The authors would like to thank the Key Laboratory of Groundwater Re-sources and Environment, Ministry of Education, Jilin University, for financial support and facilities, the National Natural Science Foundation of China for financial support, and the Oil and Gas Engineering Research Institute, CNPC Jilin Oilfield Company, for supplying field data.

Conflicts of Interest: Author Ruosheng Pan was employed by the CNPC Jilin Oilfield Company. The remaining authors declare that the research was conducted in the absence of any commercial or financial relationships that could be construed as a potential conflict of interest.

References

1. Li, Q.; Li, Q.; Li, Q.; Li, Q.; Wang, Y. The Carrying Behavior of Water-Based Fracturing Fluid in Shale Reservoir Fractures and Molecular Dynamics of Sand-Carrying Mechanism. *Processes* **2024**, *12*, 2051. [CrossRef]
2. Yu, H.; Fu, W.; Zhang, Y.; Lu, X.; Cheng, S.; Xie, Q.; Qu, X.; Yang, W.; Lu, J. Experimental study on EOR performance of CO_2-based flooding methods on tight oil. *Fuel* **2021**, *290*, 119988. [CrossRef]
3. Rajkumar, P.; Pranesh, V.; Kesavakumar, R. Influence of CO_2 retention mechanism storage in Alberta tight oil and gas reservoirs at Western Canadian Sedimentary Basin, Canada: Hysteresis modeling and appraisal. *J. Pet. Explor. Prod. Technol.* **2021**, *11*, 327–345. [CrossRef]
4. Song, X.; Wang, F.; Ma, D.; Gao, M. Progress and outlook of CO_2 capture, oil drive and burial technology for petroleum in China. *Pet. Ex-Ploration Dev.* **2023**, *50*, 206–218.
5. Hu, Y.; Hao, M.; Chen, G.; Sun, R. Technology and practice of CO_2 oil drive and burial in China. *Pet. Explor. Dev.* **2019**, *46*, 716–727.
6. Ji, B.; Wang, Y.; Nie, J.; Zhang, L. Research progress and application of enhanced recovery technology in Sinopec. *Oil Gas. Geol.* **2016**, *37*, 572–576.

7. Yuan, S.; Wang, Q.; Li, J.; Han, H. Technology progress and prospects of enhanced oil recovery by gas injection. *Acta Pet. Sin.* **2020**, *41*, 1623–1632.
8. Jia, J. *Numerical Simulation of CO_2 Miscible Flooding in Heterogeneous and Anisotropic Porous Media*; Dalian University of Technology: Dalian, China, 2022. [CrossRef]
9. Hopkinson, J.L.; Natanson, S.G.; Temple, A.P. Effects of Reservoir Heterogeneity on Performance. In Proceedings of the Society of Petroleum Engineers—Fall Meeting of the Society of Petroleum Engineers of AIME, Denver, CO, USA, 2–5 October 1960.
10. Weber, K.J. How heterogeneity affects oil recovery. *Reserv. Charact.* **1986**, 487–544.
11. Khataniar, S.; Peters, E.J. The effect of reservoir heterogeneity on the performance of unstable displacements. *J. Pet. Sci. Eng.* **1992**, *7*, 263–281. [CrossRef]
12. Yang, S.C. A new method for quantitatively studying reservoir heterogeneity. *J. Univ. Pet. China* **2000**, *24*, 53–56.
13. Wang, G.; Yang, S.C.; Liao, F. Reservoir Heterogeneity and Remaining Oil Distribution of Debouch Bar Reservoir. *Fault -Block Oil Gas. Field* **2006**, *13*, 18–19.
14. Shedid, S. Influences of different modes of reservoir heterogeneity on performance and oil recovery of carbon dioxide miscible flooding. *J. Can. Pet. Technol.* **2009**, *48*, 29–36. [CrossRef]
15. Guo, K.; Zeng, J.; Lu, X.; Cui, Z.; Shi, Y. An Experimental Study of Oil Migration Controlled by Vertical Conduction of Faults and Reservoir Heterogeneity. *Geoscience* **2010**, *24*, 1164–1170.
16. Wang, J.; Xie, J.; Lu, H. CO_2 miscible flooding influence degree analysis of reservoir heterogeneity in low permeability reservoir. *Int. J. Oil Gas Coal Technol.* **2016**, *13*, 142–158. [CrossRef]
17. Hadipoor, M.; Taghavi, H.; Taghavi, H. Experimental investigation of CO_2 injection performance in heterogeneous reservoirs: Parametric analysis. *Pet. Sci. Technol.* **2020**, *38*, 837–848. [CrossRef]
18. Wang, C. Investigation on the Influence of Reservoir Heterogeneity on CO_2 Flooding. Master's Thesis, China University of Petroleum, Beijing, China, 2019.
19. Dong, Y.; Li, J.; Wu, X.; Mei, Y. Study on Effect of Reservoir Heterogeneity on CO_2 Flooding. *Contemp. Chem. Ind.* **2016**, *45*, 2370–2373.
20. Liao, H.; Lv, C.; Zhao, S.; Chen, Y.; He, Y.; Zhou, Y.; Wang, Q. Numerical simulation to study the influence factors of CO_2 drive in low-permeability reservoirs. *Xinjiang Pe-Troleum Geol.* **2011**, *32*, 520–522.
21. Zhang, L.; Kuang, X.; Li, J. Numerical simulation of CO_2 gas drive in inhomogeneous reservoir. *China New Technol. Prod.* **2010**, 6.
22. Zhang, M. Numerical simulation of CO_2 drive influencing factors in low-permeability oilfield of Fang 48 block. *J. Daqing Pet. Inst.* **2011**, *35*, 64–67+118.
23. Zhao, M.; Chen, X.; Jia, H.; Yang, H. Study on the effect of carbon dioxide oil repulsion in Fang 48 inhomogeneous fault block reservoir. *Spec. Oil Gas. Reserv.* **2014**, *21*, 119–122+157.
24. Liu, J. A quantitative study to investigate the effect of reservoir inhomogeneity on CO_2 oil-driving efficiency in medium- and high-permeability extra-high water-bearing reservoirs. *China Chem. Trade* **2017**, *9*, 203.
25. Kang, W.-L.; Zhou, B.-B.; Issakhov, M.; Gabdullin, M. Advances in enhanced oil recovery technologies for low permeability reservoirs. *Pet. Sci.* **2022**, *19*, 1622–1640. [CrossRef]
26. Jia, K.; Cui, C.; Wu, Z.; Yan, D. Influences of Reservoir Heterogeneity on Gas Channeling During CO_2 Flooding in Low Permeability Reservoirs. *Xinjiang Pet. Geol.* **2019**, *40*, 208–212.
27. Zhang, S.; Shi, L.; Kang, K.; Wang, W.; Wang, X. Influence law of heterogeneity on CO_2 driven gas flushing in low/extra-low permeability reservoirs and ex-perimental study of plugging. *Deilling Prod. Technol.* **2018**, *41*, 69–72.
28. Liu, B.; Liu, Y. Evaluation of carbon dioxide flooding effect based on reservoir heterogeneity. *Chem. Eng.* **2017**, *31*, 40–42+33.
29. Zhang, L.; Li, X.; Ren, B.; Cui, G.; Zhang, Y.; Ren, S.; Chen, G.; Zhang, H. CO_2 storage potential and trapping mechanisms in the H-59 block of Jilin oilfield China. *Int. J. Greenh. Gas. Control* **2016**, *49*, 267–280. [CrossRef]
30. Ren, B.; Ren, S.; Zhang, L.; Chen, G.; Zhang, H. Monitoring on CO_2 migration in a tight oil reservoir during CCS-EOR in Jilin Oilfield China. *Energy* **2016**, *98*, 108–121. [CrossRef]
31. Liu, Q. Research on Optimization Technology of Lithological Reservoir Enrichment in Daqingzijing Oilfield. Master's Thesis, Northeast Petroleum University, Daqing, China, 2015.
32. Li, Y. Philosophy of Daqingzijing Oilfield Development in Jilin. *Unconventonal Oil Gas.* **2016**, *3*, 88–92.
33. Sun, R.; Ma, X.; Wang, S. Process technology of CO_2 drive surface engineering in Jilin oilfield. *Pet. Plan. Des.* **2013**, *24*, 1–6+31+48.
34. Abou-Kassem, J.H.; Farouq-Ali, S.M.; Islam, M.R. *Petroleum Reservoir Simulations*; Elsevier: Amsterdam, The Netherlands, 2013.
35. Li, Y.; Xu, T.; Xin, X.; Yang, B.; Xia, Y.; Zang, Y.; Yuan, Y.; Zhu, H. Pore-scale study of the dynamic evolution of multi-phase seepage parameters during hydrate dissociation in clayey silt hydrate-bearing sediments. *J. Hydrol.* **2024**, *635*, 131178. [CrossRef]
36. Steffen, M. A simple method for monotonic interpolation in one dimension. *Astron. Astrophys.* **1990**, *239*, 443.
37. Pan, L.; Oldenburg, C.M. *TOGA: A Tough Code for Modeling Three-Phase, Multi-Component, and Non-Isothermal Processes Involved in CO_2-Based Enhanced Oil Recovery*; Lawrence Berkeley National Lab: Berkeley, CA, USA, 2016.
38. Lei, H. Deposition Mechanisms and Reservoir Protection Countermeasures of a Low-Permeability Formation in CO_2 Flooding Process. Ph.D. Thesis, China University of Petroleum, Beijing, China, 2017.
39. Shi, H.; Bai, Y.; Dong, W. Feedstock Components into a Virtual Method. *Guangzhou Chem. Ind.* **2009**, *37*, 114–117.
40. Hu, T. *Study on the Process Model of CO_2 Migration and Phase Transformation in Enhanced Oil Recovery System*; Jilin University: Jilin, China, 2022. [CrossRef]

41. Tian, H.; Pan, F.; Xu, T.; McPherson, B.J.; Yue, G.; Mandalaparty, P. Impacts of hydrological heterogeneities on caprock mineral alteration and containment of CO_2 in geological storage sites. *Int. J. Greenh. Gas. Control* **2014**, *24*, 30–42. [CrossRef]
42. Vanmarcke, E.; Grigoriu, M. Stochastic finite element analysis of simple beams. *J. Eng. Mech.* **1983**, *109*, 1203–1214. [CrossRef]